International Journal of Pharmaceutics 420 (2011) 266–273

Contents lists available at SciVerse ScienceDirect

International Journal of Pharmaceutics

journal homepage: www.elsevier.com/locate/ijpharm

In vivo release of bovine serum albumin from an injectable small intestinal submucosa gel

Kkot Nim Kang[a], Da Yeon Kim[a], So Mi Yoon[a], Jin Seon Kwon[a], Hyo Won Seo[a], E Sle Kim[a], Bong Lee[b], Jae Ho Kim[a], Byoung Hyun Min[a], Hai Bang Lee[a], Moon Suk Kim[a,*]

[a] Department of Molecular Science and Technology, Ajou University, Suwon 443-749, Republic of Korea
[b] Department of Polymer Engineering, Pukyong National University, Busan 608-739, Republic of Korea

ARTICLE INFO

Article history:
Received 4 July 2011
Received in revised form 1 August 2011
Accepted 28 August 2011
Available online 2 September 2011

Keywords:
Small intestine submucosa
Injectable
Gel
BSA
Protein

ABSTRACT

We aimed to develop a delivery system capable of maintaining a sustained release of protein drugs at specific sites using potentially biocompatible biomaterials. Here, we used bovine serum albumin (BSA) as a test protein to explore the potential utility of an injectable small intestine submucosa (SIS) as a depot for protein drugs. The prepared SIS powder was dispersed in PBS. The SIS suspension easily entrapped BSA in pharmaceutical formulations at room temperature. When this was suspension subcutaneously injected into rats, it gelled, forming an interconnecting three-dimensional network SIS structure to allow BSA to penetrate through it. The amount of BSA-FITC released from the SIS gel was determined in rat plasma and monitored by real-time *in vivo* molecular imaging. The data indicated the sustained release of BSA-FITC for 30 days *in vivo*. In addition, SIS gel provoked little inflammatory response. Collectively, our results show that the SIS gel described here could serve as a minimally invasive therapeutics depot with numerous benefits compared to other injectable biomaterials.

1. Introduction

The success of any therapeutic protein drug delivery depends not only upon improving its bioactivity, but also on improving its bioavailability in the human body (Tiwari et al., 2010; Shegokar and Müller, 2010). Although several drug delivery strategies have been focused on systems to improve bioactivity and bioavailability, none have proved fully satisfactory due to limitations posed by the sensitivity of protein structures in biological environments. Thus, there is a need for delivery systems that are capable of maintaining the therapeutic efficacy of protein drugs inside various extracellular matrices for predefined periods, from one or more times a week to monthly or longer intervals at specific action sites, thereby improving bioactivity and bioavailability (Lee et al., 2008; Uebersax et al., 2009).

One such approach is the use of an injectable drug depot, which achieves greater therapeutic efficacy of protein drugs than does conventional drug delivery via oral or intravenous routes. Various injectable drug depots, like those using collagen, gelatin, hyaluronate, cellulose, and fibrin, as well as synthetic materials, have been developed for this purpose (Kim et al., 2011; Kang et al., 2010; Lee et al., 2010; Yang et al., 2009; Yu and Ding, 2008; Lupton and Alster, 2000). Among them, collagen has the advantage of mimicking many features of the extracellular matrix (ECM) of mammals and it has high mechanical strength, good biocompatibility, low antigenicity, and water-uptake properties (Bhang et al., 2009; Kim et al., 2009; Ruozi et al., 2009; Pollack, 1999; Wallace and Rosenblatt, 2003). In addition, collagens easily flow in biological mediums, suggesting the possibility of it acting as an easily injectable drug depot (Wallace and Rosenblatt, 2003).

Small intestine submucosa (SIS), derived from the submucosal layer of porcine intestine, is also an ECM and consists of types I and III collagens, which together comprise greater than 90% of the total collagen content; small amounts of types IV, V, and VI collagens also are present in addition to several biologic factors (Badylak, 2007; Cheng and Kropp, 2000). It is widely known as an ideal biomaterial because of its good biocompatibility and non-immunogenic property (Badylak, 2007).

Recently, a broad range of biomedical products based on SIS have been developed and commercialized (Badylak, 2007). Recently, we investigated SIS sheets and sponges for use as scaffolds for tissue engineering (Ahn et al., 2007; Kim et al., 2006, 2007a,b, 2010). SIS could be prepared as a SIS suspension via SIS powder through a variety of processing steps, including mechanical manipulation, digestion, and sterilization. Ideally, the SIS suspension would be easily used for pharmaceutical formulations by simply mixing it with the therapeutic protein drug. When injected by syringe at the target location, this protein-loaded SIS suspension can form a

* Corresponding author. Tel.: +82 31 219 2608; fax: +82 31 219 3931.
E-mail address: moonskim@ajou.ac.kr (M.S. Kim).

0378-5173/$ – see front matter © 2011 Elsevier B.V. All rights reserved.
doi:10.1016/j.ijpharm.2011.08.047

protein-loaded SIS gel that acts as a depot for sustained delivery of the protein drug.

The overall aim of the current study was to develop a biocompatible drug carrier capable of serving as depots for protein drugs. To the best of our knowledge, the SIS-based protein drug carrier acting as *in vivo* drug depots is at the early stages of research (Freytes et al., 2008). In this study, we prepared bovine serum albumin-fluorescein isothiocyanate (BSA-FITC) – loaded SIS suspensions. We wanted to assess the *in vivo* release of BSA-FITC as a model protein and to evaluate the formation of drug depots *in vivo* by administering the BSA-FITC – loaded SIS suspension subcutaneously to rats. Our second aim was to characterize the host tissue response to determine whether BSA-FITC – loaded SIS gels could be used for sustained *in vivo* protein delivery.

2. Materials and methods

2.1. Preparation of SIS suspension

Sections of porcine jejunum were harvested from market pigs (Finish pig, F_1; Land race + Yorkshire, around 100 kg at 6 months) within 4 h of sacrifice and they were prepared according to the method of our previous work (Kim et al., 2006). Briefly, to separate SIS in porcine jejunum, fat was first removed from the porcine jejunum, followed by careful washing with water. The porcine jejunum was cut in lengths of approximately 10 cm and then washed with a saline solution. SIS was obtained by mechanical removal of the tunica serosa and tunica muscularis. Finally, the obtained SIS was washed again with a saline solution and it was freeze–dried at −80 °C for 48 h using a freeze dryer (FD 8505, Ilshinlab, Daejeon, Korea). The dried SIS was pulverized using a freezer mill (6700, SPEX Inc., USA) at −198 °C to yield 10∼20 μm size SIS powder. The obtained SIS powders were added to 10 mL vials with an aqueous solution consisting of 3% acetic acid and 0.1% pepsin, and then stirred for 48 h. The solution was followed by freeze-drying to yield the final SIS powders. The SIS powder was sterilized using ethylene oxide (EO) gas. The SIS powder was dispersed in PBS to yield the desired concentrations (10, 15, and 20 wt%) of SIS. The final SIS suspension was a translucent emulsion-sol form. Viscosity measurements of 10, 15, and 20 wt% SIS suspension were performed using a Brookfield DV-III ultra viscometer equipped with a programmable rheometer and circulating baths with a programmable controller (TC-502P, Brookfield Engineering Laboratories, Middleboro, MA). The viscosity of suspension was investigated using a T-F spindle rotating at 0.2 rpm at 37 °C.

2.2. In vivo gel formation and protein release

Twenty-four 8-week-old Sprague-Dawley rats (320–350 g), divided into two groups (BSA-FITC-loaded SIS gel for twenty-one rats and BSA–FITC solution for only three rats), were used in the *in vivo* release tests. All animals were treated in accordance with the Ajou University School of Medicine Animal Care Guidelines. Three formulation types of BSA-FITC-loaded SIS suspension and BSA–FITC only solution (containing 1 mg/mL BSA-FITC) were individually injected into each rat for each formulation for the *in vivo* release experiments. Within 30 minutes of adding BSA-FITC to the SIS suspensions, 0.5 mL of the solution was injected subcutaneously (1 cc syringe, 21-gauge needle) into the dorsum of a rat anesthetized with ethyl ether.

For the *in vivo* detection of BSA-FITC, an aliquot of blood was drawn from the tail vein of each rat at specified times. A 0.3-mL aliquot of blood from the catheterized tail vein was collected into a microfuge tube, mixed with 0.2 mL of a 1:499 mixture of heparin and saline, and vortexed. Plasma was obtained by centrifuging the blood solution at 10,000 rpm for 5 min at room temperature. Distilled water (100 μL), 66 mM EDTA (300 μL), and 50 mM HEPES, pH 7.4 (400 μL), were added to the plasma. The obtained sample was immediately analyzed by fluorescence spectroscopy (F-6500, Jasco, Tokyo, Japan). To analyze the state of the probe and to assess the reliability of the method, we recorded the fluorescence spectra of solutions of BSA-FITC in plasma containing known concentrations of BSA-FITC using an excitation wavelength of 490 nm with a bandwidth of 3 nm, an emission wavelength of 525 nm with a bandwidth of 3 nm, and a response time of 2 s. The amount of BSA-FITC cumulatively released by the BSA-FITC-loaded SIS gels was calculated by reference to standard calibration curves prepared with known concentrations of BSA-FITC. The release experiment was performed separately on each group, and the results were averaged. The amount of BSA-FITC remaining at predetermined times was measured in individual gels removed from the sacrificed rats. Gels were first dissolved in distilled water (5 mL) and then filtered. The amount of remaining BSA-FITC was calculated by reference to standard calibration curves prepared with known concentrations of BSA-FITC in deionized water.

2.3. Scanning electron microscopy of in vivo gels

The morphology of the *in vivo*-formed gels was examined by scanning electron microscopy (SEM) using a JSM-6380 SEM (JEOL, Tokyo, Japan). Immediately after removing a sample from a rat, the gel samples were mounted on a metal stub pre-cooled in liquid nitrogen. After mounting the gel, the metal stub was quickly immersed in a liquid nitrogen bath to minimize alterations of the gel. The stub was then freeze–dried at −75 °C using a freeze dryer, coated with a thin layer of gold using a plasma-sputtering apparatus (Ted Pella, Cressington 108 Auto, CA, USA) under an argon atmosphere, and examined by SEM.

2.4. In vivo fluorescence imaging

Three formulation types of SIS suspension containing 1 mg/mL BSA-FITC and SIS suspension only were prepared and injected subcutaneously into the left dorsum of a 6-week old male nude mouse (anesthetized with ethyl ether) using a 21-gauge needle. At selected times, side-view images of the mouse were collected at a wavelength of 515 nm (excitation wavelength, 470 nm) using a fluorescence imaging system (FO ILLUM PL-800, Edmund Optics, NJ, USA, 150 W EKE Quartz Halogen light, glass reference number OG515 filter). After digitization using a charge-coupled device (CCD), fluorescence images were visualized with Axiovision Rel. 4.8 software.

2.5. Histological analysis

At 1, 5, and 10 days after implantation, the rats were sacrificed and the gels were individually dissected and removed from the subcutaneous dorsum. The tissues were immediately fixed with 10% formalin and embedded in paraffin. The embedded specimens were sectioned (4 μm) along the longitudinal axis of the implant, and the sections were stained with hematoxylin and eosin (H&E), 4′,6-diamino-2-phenylindole dihydrochloride (DAPI, Sigma–Aldrich, St Louis, MO, USA) and mouse anti-rat CD68 antibody macrophage marker (ED1; 1:1000; Serotec, Oxford, UK). The staining procedures for DAPI and ED1 were as follows. The slides were washed with PBS-T (0.05% Tween 20 in PBS), and blocked with 5% bovine serum albumin (BSA; Bovogen, Melbourne, Australia) and 5% horse serum (HS; GIBCO, Paisley, UK) in PBS for 1 h at 37 °C. The sections were incubated overnight at 4 °C with the ED1 antibodies,

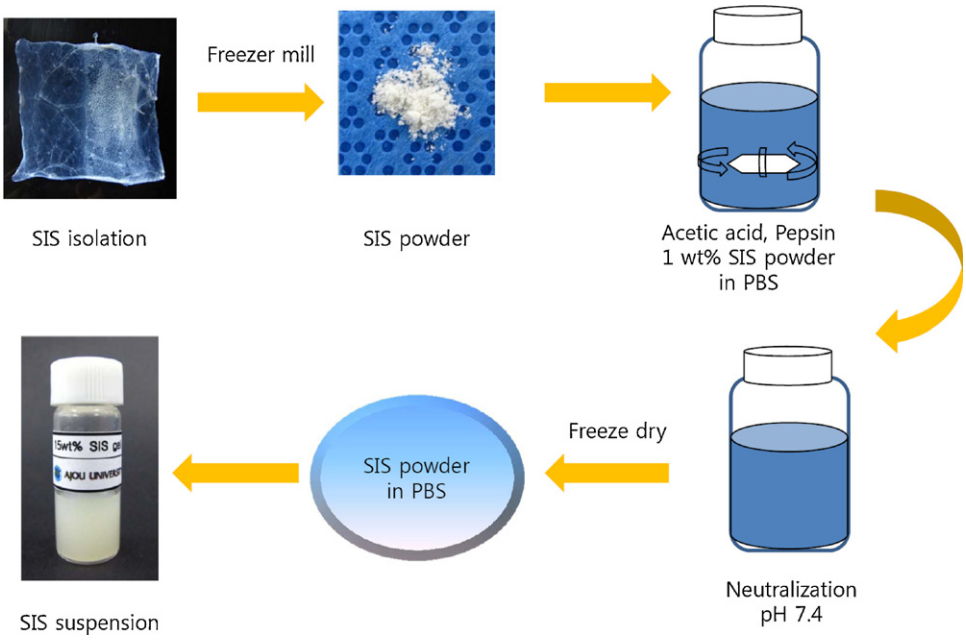

Fig. 1. Schematic diagram for the preparation of the SIS suspension.

washed with PBS-T, and then incubated with the secondary antibody (goat anti-mouse Alexa Fluor® 594; Invitrogen, San. Diego, CA, USA) for 3 h at room temperature in the dark. The slides were washed again with PBS-T, counterstained with DAPI, and then mounted with a fluorescent mounting solution (DAKO, Calif, USA). Immunofluorescent images were obtained using an Axio Imager A1 (Carl Zeiss Microimaging GmbH, Göttingen, Germany) and analyzed with Axiovision Rel. 4.8 software (Carl Zeiss Microimaging GmbH). Before the visualization of immunofluorescence images, the delimitation between gel and host tissue was determined from the image of the optical microscopy with digital camera (DIC).

2.6. Statistical analysis

ED1 assays of SIS gel were carried out in independent experiments with $n = 9$ for each data point, with data given as the mean and standard deviation (SD). The results were analyzed with one way-ANOVA using the Prism 3.0 software package (GraphPad Software Inc., San Diego, CA, USA).

3. Results

3.1. Preparation of SIS suspension

A schematic diagram of the SIS suspension is represented in Fig. 1. The inside and outside layer of the porcine jejunum was removed mechanically and was then freezer milled to yield SIS fine powder with a size range of approximately 10–20 μm. The SIS powder was only swelling in water as well as in a biological solution and was not soluble, so the SIS powder was added to an aqueous mixture solution of acetic acid and pepsin, and stirred to cleave only non-triplehelical domains of collagen. The collagen molecules which had native triplehelical structures were solubilized from tissue. Accordingly, the suspension of SIS powder changed to a swelled form after 24 h and finally a SIS suspension was made after 48 h. The suspension of SIS was neutralized to prevent the acid inflammation. The SIS suspensions of 10, 15, and 20 wt% SIS were prepared in PBS. All SIS suspensions were translucent emulsion–sol forms.

3.2. Viscosity of SIS suspension

To gain an understanding for the concentration-dependent of SIS suspension, we examined the viscosity of SIS suspensions of 10, 15, and 20 wt% at 37 °C. The maximum viscosities of SIS suspensions of 10, 15, and 20 wt% were 2.5×10^3 cP, 3.8×10^3 cP, and 1.0×10^4 cP, respectively. This demonstrates that the SIS gels may become more tightly as the concentration is increased.

3.3. In vivo gelation

We injected an SIS suspension into Fisher rats to test its utility as an *in vivo* depot for BSA (Fig. 2). The SIS suspension gelled in the rat that was subjected to subcutaneous (s.c.) injection (Fig. 2a). The resulting *in situ*-formed gel was allowed to develop *in vivo* and was biopsied after implantation. The injected SIS gel maintained its shape at the injection site for the full experimental observation period. Following removal of the gel at 14 days (Fig. 2b), a jelly form was obtained (Fig. 2c). These results indicate that the BSA-FITC-loaded SIS gels maintained sufficient structural integrity to act as a drug depot *in vivo*.

3.4. Morphology of the in vivo-formed SIS gel

To investigate the morphology of the *in vivo*-formed gel, we removed a SIS gel from one rat 7 days after s.c. injection. The gel was frozen in liquid nitrogen, freeze-dried, and observed by SEM (Fig. 3). SEM micrographs of the gel cross-section indicated that it consisted of two layers: a dense outer region and an inner region with an interconnected structure with a pore diameter of 10–50 μm. The SIS gel that formed *in vivo* exhibited a structure sufficiently porous to not only allow biological medium to diffuse into and out of the gel, but also to enable BSA to pass out of the gel. These observations provide further support for *in vivo*-formed SIS gel's capability as a candidate for an *in vivo* protein drug depot.

3.5. In vivo release

To determine the *in vivo* BSA-FITC release, we prepared a BSA-FITC-only solution (1 mg/mL) and BSA-FITC-loaded SIS

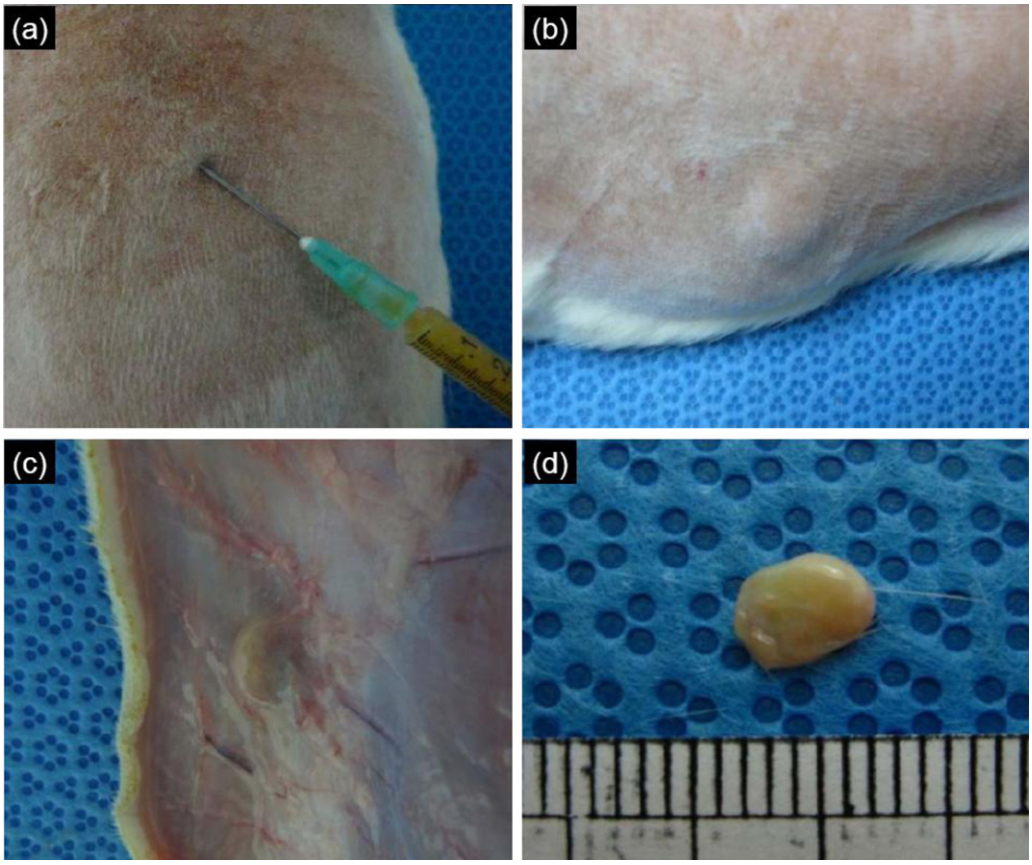

Fig. 2. Subcutaneous injection of SIS suspension (a), formed gel (b, c), and (d) removed gels from a rat after 2 weeks.

suspension using different SIS concentrations (10, 15, and 20 wt%) with BSA-FITC (1 mg/mL), and injected them into rats. BSA-FITC was allowed to release from BSA-FITC-loaded SIS gels *in vivo* for 20 days and was monitored by measuring the plasma of the BSA-FITC concentrations using fluorescence spectroscopy. Fig. 4 shows a plot of the plasma BSA-FITC concentration versus time.

In rats injected with the BSA-FITC-only solution, the plasma BSA-FITC concentrations reached a maximum 5 h after s.c. injection and then rapidly declined, approaching zero after 1 day. In contrast, plasma BSA-FITC concentrations in rats injected with a BSA-FITC-loaded SIS suspension reached a maximum at 9 h, but exhibited a sustained-release profile, producing detectable levels of BSA-FITC in plasma for up to 20 days.

The T_{max}, C_{max}, and absolute bioavailability data, calculated from Fig. 4, are summarized in Table 1. The T_{max} and C_{max} values of the BSA-FITC-loaded SIS gel were significantly higher and lower than those for the BSA-FITC-solution only, respectively. In addition, the C_{max} values decreased as the SIS concentration increased. AUC_{0-t} values were calculated by measuring the area under the plasma BSA-FITC curves from t_0 to time t using the trapezoidal rule, and the relative bioavailability of BSA-FITC was determined from the plasma concentration profiles. The AUC_{0-t} values were 27, 45, and 52 μg/mL for BSA-FITC-loaded SIS gels prepared with 10, 15, and 20 wt% SIS, respectively. The relative bioavailability of BSA-FITC from SIS gels prepared with 10, 15, 20 wt% SIS was 101%, 227%, and 234% of the AUC_{0-t} for the BSA-FITC-only solution at these same BSA-FITC concentrations. The T_{max}, C_{max}, and bioavailability depended on the SIS concentration. This result indicates that BSA-FITC-loaded SIS gels were capable of sustained and effective release of BSA-FITC.

3.6. *In vivo* fluorescence imaging

We used real-time molecular imaging, which has been shown to be effective for assessing *in vivo* drug release processes in live animals, in order to evaluate *in vivo* BSA-FITC release. Fluorescent images were acquired from a nude mouse after s.c. injection of a BSA-FITC-loaded SIS suspension with and without BSA-FITC (Fig. 5). There is no green fluorescence image in the SIS suspension without BSA-FITC (Fig. 5a) for live mice and even in the removed gel (Fig. 5b and c). This indicates that the SIS gel did not yield a self-fluorescence image.

Meanwhile, the s.c. injection of the BSA-FITC-loaded SIS suspension exhibited a green fluorescence image at the injection site (Fig. 5d). The area of fluorescence gradually increased and thereafter, reached a maximum area around 5–12 h after administration. After 24 h, both the intensity and area of the fluorescence image gradually decreased. The green fluorescence image was sustained for 4 weeks. Even though the plasma BSA-FITC concentration after 20 days dropped to zero due to the detection limits of the fluorescence spectroscopy, a negligible *in vivo* fluorescence image was observed even after 28 days. This result indicated that BSA-FITC release was sustained after administration of BSA-FITC-loaded SIS gels.

3.7. Host tissue response

BSA-FITC-loaded SIS gels injected into rats could be easily identified and isolated from the surrounding tissue. To assess the local biocompatibility of the SIS gel, we examined tissues surrounding the area into which the SIS gel had been transplanted. After 1,

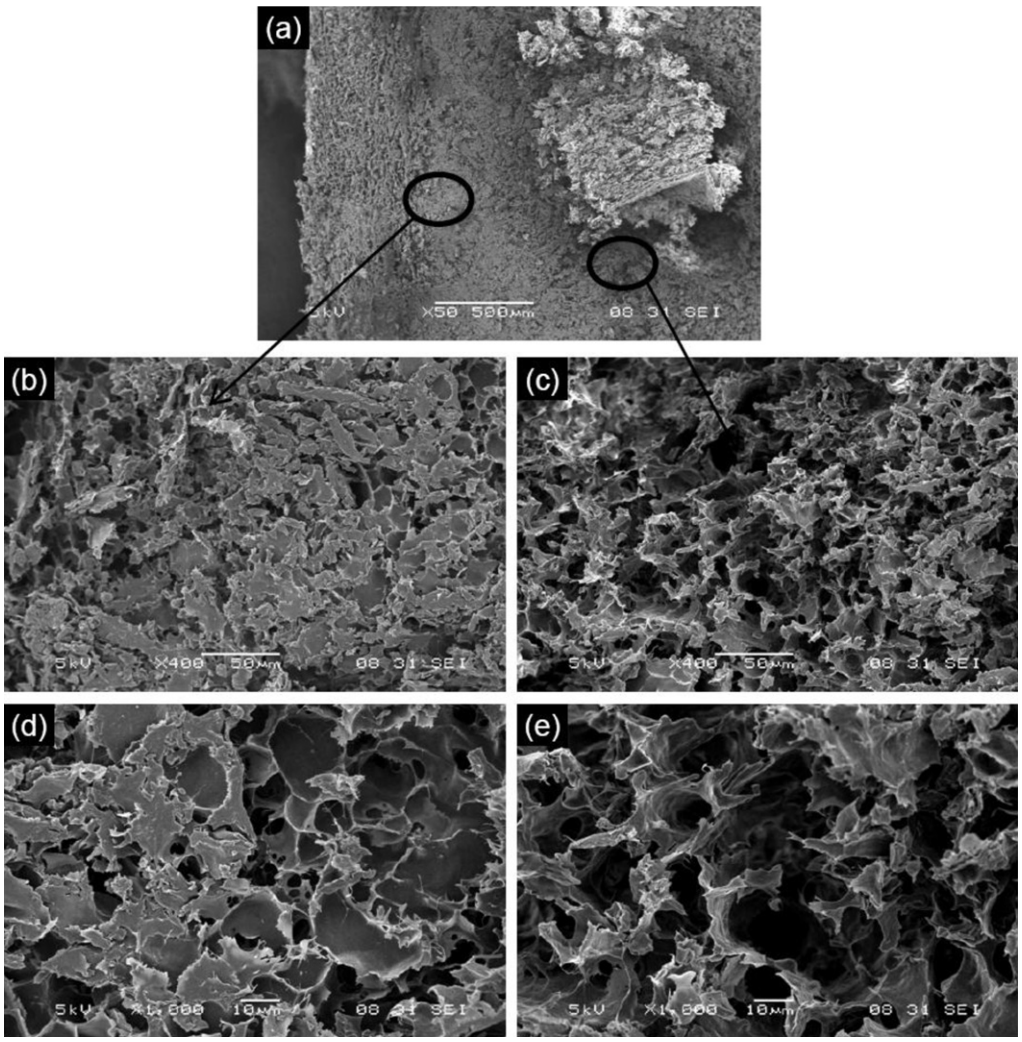

Fig. 3. SEM micrographs showing the morphology of an *in vivo*-formed SIS gel after 7 days. (a), (b, d), and (c, e) represent images of whole, outer, and inner regions, respectively. Magnification: (a) 50×, (b, c) 400×, (d, e) 1000×.

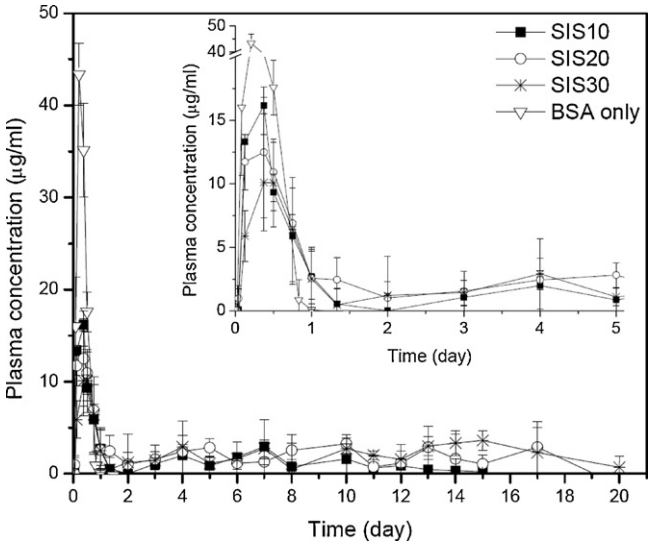

Fig. 4. Time course of BSA-FITC concentration in plasma over 20 days after s.c. injection of BSA-FITC-only solution only and BSA-FITC-loaded SIS prepared with 10, 15, and 20 wt% SIS.

5, and 10 days, the extent of host cell infiltration and inflammatory cell accumulation within and near the transplanted SIS gel was characterized by H&E and ED1-stained tissue (Fig. 6). A few macrophages, neutrophils, and/or lymphocytes and new blood vessels were observed in the H&E staining tissue. In the staining tissue with the ED1 antibody and the nuclear DAPI stain, ED1 staining (red) had a few macrophages near the SIS gel and in the surrounding tissues after 1, 5, and 10 days. Positive ED1 staining (red) of the harvested SIS gel was observed in the border zone and near the SIS gel. The ED1-positive cells were counted and normalized to the total stained tissue area in order to determine the extent of inflammation (Fig. 7). Significantly less macrophage was observed in the SIS gel even at 1 day. In addition, the macrophages decreased from 12% to 6%.

4. Discussion

The emerging and promising next generation of injectable drug depot relies on the production of biocompatible carriers to mimic the ECM of mammals (Badylak et al., 2009; Freytes et al., 2008). Thus, it is necessary to examine the extracellular matrix as the *in situ* drug depot for a protein drug *in vivo*. SIS is an acellular, collagenous extracellular matrix material derived from the submucosa of porcine small intestine and it has various bioactive molecules (Badylak, 2007; Cheng and Kropp, 2000). Despite the good results of

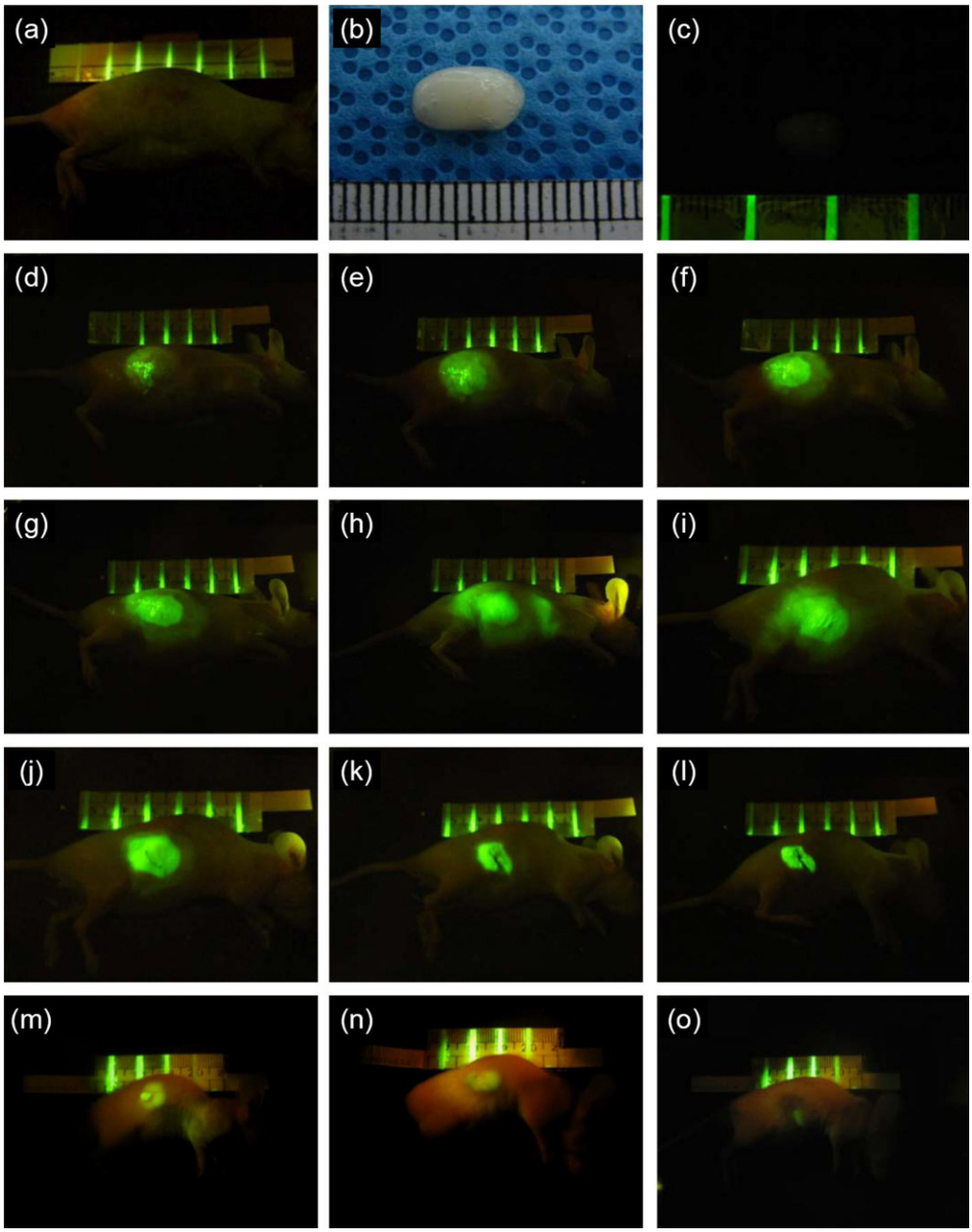

Fig. 5. *In vivo* fluorescent image of a nude mouse injected with (a) SIS suspension only, (b) removed gel, and (c) fluorescent image of the removed gel; also, *in vivo* fluorescent image of a nude mouse injected with BSA-FITC-loaded SIS suspension, taken (d) 2 min, (e) 10 min, (f) 30 min, (g) 90 min, (h) 5 h, (i) 12 h, (j) 24 h, (k) 48 h, (l) 4 day, (m) 9 days, (n) 2 weeks, and (o) 4 weeks after initial s.c. injection (Line represents 1 cm).

SIS in practical biomedical applications, few studies have evaluated the SIS suspension as a drug depot (Freytes et al., 2008).

In this work, the SIS powder was prepared through mechanical manipulation, digestion, and sterilization. The SIS powder was dispersed in PBS to form injectable suspensions of SIS. SIS suspensions are not covalent and not cross-linked. Alternatively, SIS in an injected tissue body can have viscous properties through entanglements through hydrophobic and electrostatic interactions of collagenous fibers (Wallace and Rosenblatt, 2003). This behavior is advantageous for injectable delivery, since the SIS suspension can be easily fluidized at room temperature, but become relatively rigid at body temperature. The viscosity of SIS suspension increased as the SIS concentration increased. The observation suggests that *in vivo* SIS gels may become more rigidly as the SIS concentration increased.

With respect to drug delivery, one can readily envision applications in which SIS suspensions are injected into target sites, so SIS seems to be a promising drug depot. The translucent emulsion–sol form of SIS suspension easily retains BSA as pharmaceutical formulations by physical entrapment at room temperature. Simple subcutaneous injection of the BSA-loaded SIS suspensions into rats afforded a gel. SEM images of the SIS gel showed that it has sufficiently interconnected pores. The pore network in these gels can allow permeation of the biologic medium to allow BSA to

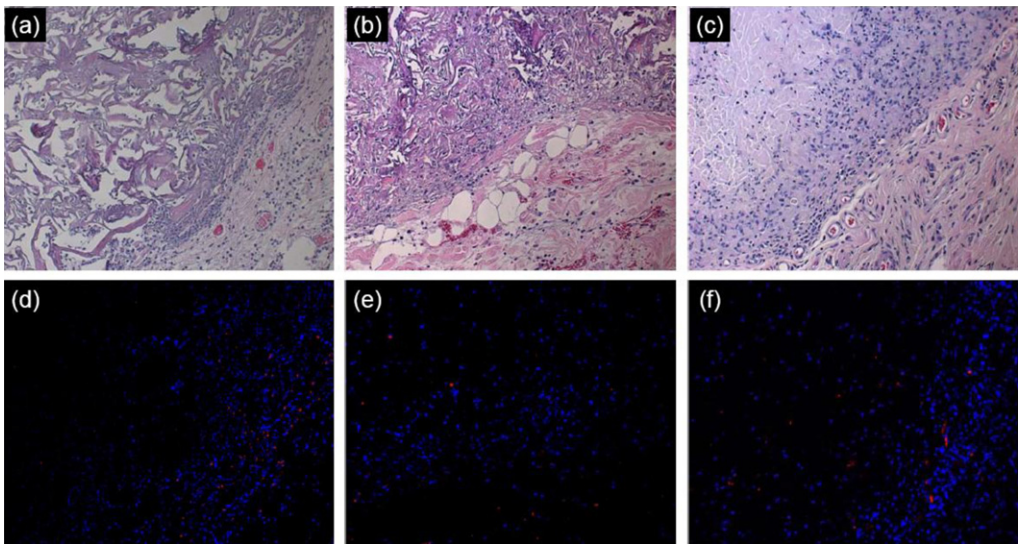

Fig. 6. H&E (a, b, c) and ED1 (d, e, f) -stained section of *in situ*-formed SIS gel after (a, d) 1 day, (b, e) 5 days, and (c, f) 10 days *in vivo*. Magnification: 200×.

Table 1
Relative bioavailabilities of BSA-FITC after subcutaneous injection of SIS and BSA-FITC-only solution containing 1 mg/mL of BSA-FITC.

Formulation	SIS concentration (mg/mL)	T_{max} (h)	C_{max}	AUC_{0-t} (μg/mL day)	Relative bioavailability[a] (%)
SIS gel	10	9	16.2 ± 0.6	27.0 ± 16.8	101.0 ± 31.0[b]
	15	9	12.5 ± 5.2	44.9 ± 19.7	227.4 ± 99.8[b]
	20	9	10.1 ± 3.8	51.5 ± 17.6	234.1 ± 89.3[b]
BSA-FITC solution only	–	5	43.4 ± 3.4	19.7 ± 0.3	100

[a] Relative Bioavailability (%) = [(AUC value for each gel administration)/(mean AUC value for BSA solution only administration)] × 100.
[b] $P < 0.05$ vs BSA-FITC solution only.

penetrate through it. This injectable property strongly suggests that SIS is suitable for use as a minimally invasive therapeutic protein drug carrier.

The release of the BSA solution lasted for only 2 days. Meanwhile, in the release test of BSA from the *in vivo* SIS gels, SIS gels showed an initial burst in their release profiles. This initial burst was possibly due to the high BSA concentration gradient between the gel surface and the surrounding tissue for the initial stage during and after injection, since the concentration gradient after gelation is the driving force for BSA diffusion (Chen et al., 2009; Ye et al., 2010). Then, the prolonged release of BSA was observed from the SIS gels for longer than 20 days. Thus, the T_{max}, C_{max}, and bioavailability values were significantly different for the injection of BSA-loaded SIS suspension and BSA only solution. The bioavailability values increased as the SIS concentration increased. The *in vivo* release of BSA from the 20 wt% SIS gel was sustained for longer than that of the 10 wt% SIS gel, indicating that the former gel has a higher bioavailability. These observations suggest that *in vivo*, the SIS gels may become more tightly entrapped as the SIS concentration increases due to greater hydrophobic and electrostatic interactions. This tighter entrapping, which is expected to be more pronounced for the 20 wt% gel, may retard the interactions between the biologic media and BSA or increase the interactions between the BSA and the gel network, thereby hindering BSA release. This explains the higher bioavailability of the 20 wt% gel than that of the 15 wt% gel. Although the BSA release seemed to have stopped after about 20 days due to the detection limits of the plasma BSA-FITC concentration in fluorescence spectroscopy, the sustained release of BSA from the SIS gel for 30 days was confirmed by real-time *in vivo* fluorescence imaging.

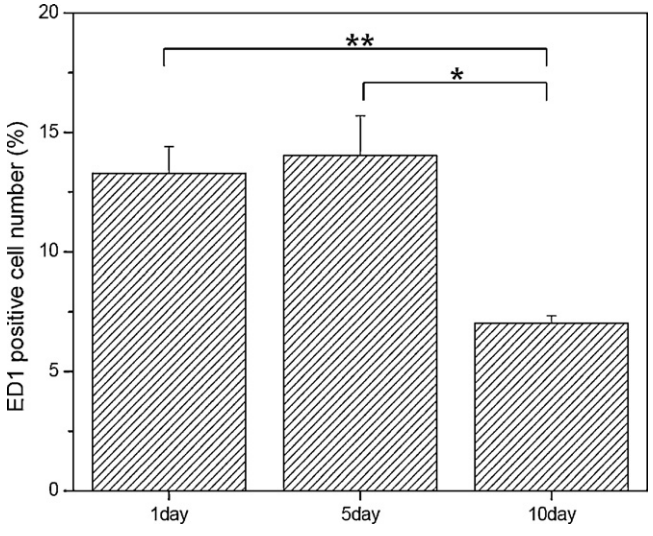

Fig. 7. The number of ED1-positive cells on SIS gel at 1, 5, and 10 days (*$P < 0.01$, *$P < 0.001$).

With the eventual goal of optimizing our SIS gel system for applications as an injectable drug depot in mind, we studied the biocompatibility of our injected SIS gels. Many cells were found scattered within the injected *in vivo* SIS gel. A number of newly formed blood vessels were also observed, demonstrating that *in vivo*-formed SIS gels might support vascular ingrowth. DAPI staining (blue) showed many host cells surrounding the SIS gel. The ED1 staining (red), which recognizes the macrophage marker CD68, is considered a unique *in vivo* indicator of an inflammatory response. ED1 staining of SIS gel (red) showed few macrophages even after 10 days. This response was significantly lower than that of the FDA-approved biomaterial, poly(lactic-co-glycolic acid) (PLGA) (Kranz et al., 2000), which promotes a substantial infiltration of macrophages and neutrophils (Lee et al., 2007; Long et al., 2006). Collectively, these results highlight the value of

in situ-formed SIS gels, showing that BSA-loaded SIS gels not only effectively sustain release of the loaded BSA, but are also biocompatible, and are therefore likely to successfully serve as drug depots.

5. Conclusion

Here, we explored the potential utility of *in situ*-formed SIS gels as drug depots. We showed that a BSA-loaded SIS suspension at room temperature gelled upon s.c. injection into rats. We also demonstrated the sustained release of BSA-FITC from the *in vivo* SIS gel over extended experimental periods. The present findings show that a SIS gel maintains its structural integrity under physiological conditions and can act as an injectable drug depot. Thus, our *in situ* gel-forming SIS system may provide numerous benefits as a minimally invasive therapeutics depot and as a useful experimental platform for testing the sustained *in vivo* pharmacological performance of protein drugs.

Acknowledgements

This study was supported by a grant from MKE (grant no. 10038665) and Priority Research Centers Program (2010-0028294) through NRF funded by the Ministry of Education, Science and Technology.

References

Ahn, H.H., Kim, K.S., Lee, J.H., Lee, M.S., Song, I.B., Kim, M.S., Khang, G., Lee, H.B., 2007. Porcine small intestinal submucosa sheets as a scaffold for human bone marrow stem cells. Int. J. Biol. Macromol. 41, 590–596.

Badylak, S.F., 2007. The extracellular matrix as a biologic scaffold material. Biomaterials 28, 3587–3593.

Badylak, S.F., Freytes, D.O., Gilbert, T.W., 2009. Extracellular matrix as a biological scaffold material: structure and function. Acta Biomater. 5, 1–13.

Bhang, S.H., Lee, T.J., Lim, J.M., Lim, J.S., Han, A.M., Choi, C.Y., Kim, Y.H., Kim, B.S., 2009. The effect of the controlled release of nerve growth factor from collagen gel on the efficiency of neural cell culture. Biomaterials 30, 126–132.

Chen, L., Wu, J., Yuwen, L., Shu, T., Xu, M., Zhang, M., Yi, T., 2009. Inclusion of tetracycline hydrochloride within supramolecular gels and its controlled release to bovine serum albumin. Langmuir 25, 8434–8438.

Cheng, E.Y., Kropp, B.P., 2000. Urologic tissue engineering with small-intestinal submucosa: potential clinical applications. World J. Urol. 18, 26–30.

Freytes, D.O., Martin, J., Velankar, S.S., Lee, A.S., Badylak, S.F., 2008. Preparation and rheological characterization of a gel form of the porcine urinary bladder matrix. Biomaterials 29, 1630–1637.

Lee, E.S., Park, K.H., Kang, D., Park, I.S., Min, H.Y., Lee, D.H., Kim, S., Kim, J.H., Na, K., 2007. Protein complexed with chondroitin sulfate in poly(lactide-co-glycolide) microspheres. Biomaterials 28, 2754–2762.

Lee, J.Y., Kim, K.S., Lee, J.H., Hwang, S.J., Lee, B., Khang, G., Lee, H.B., Kim, M.S., 2008. A recent tendency of protein drug delivery system for bioefficacy improvement. Tissue Eng. Regen. Med. 5, 587–593.

Lee, J.Y., Kim, K.S., Kang, Y.M., Kim, E.S., Hwang, S., Lee, H.B., Min, B.H., Kim, J.H., Kim, M.S., 2010. In vivo efficacy of paclitaxel-loaded injectable in situ-forming gel against subcutaneous tumor growth. Int. J. Pharm. 392, 51–56.

Long, R.A., Nagatomi, J., Chancellor, M.B., Sacks, M.S., 2006. The role of MMP-I upregulation in the increased compliance in muscle-derived stem cell-seeded small intestinal submucosa. Biomaterials 27, 2398–2404.

Lupton, J.R., Alster, T.S., 2000. Cutaneous hypersensitivity reaction to injectable hyaluronic acid gel. Dermatol. Surg. 26, 135–137.

Kang, Y.M., Lee, S.H., Lee, J.Y., Son, J.S., Kim, B.S., Lee, B., Chun, H.J., Min, B.H., Kim, J.H., Kim, M.S., 2010. A biodegradable, injectable, gel system based on MPEG-b-(PCL-ran-PLLA) diblock copolymers with an adjustable therapeutic window. Biomaterials 31, 2453–2460.

Kim, M.S., Kim, J.H., Min, B.H., Chun, H.J., Han, D.K., Lee, H.B., 2011. Polymeric scaffolds for regenerative medicine. Polym. Rev. 51, 23–52.

Kim, K.S., Lee, J.Y., Kang, Y.M., Kim, E.S., Kim, G.H., Rhee, S.D., Cheon, H.G., Kim, J.H., Min, B.H., Lee, H.B., Kim, M.S., 2010. Small intestine submucosa sponge for *in vivo* support of tissue-engineered bone formation in the presence of rat bone marrow stem cells. Biomaterials 31, 1104–1113.

Kim, K.H., Kim, M.H., Lim, Y.H., Park, S.R., Choi, B.H., Park, H.C., Yoon, S.H., Min, B.H., Park, H., 2009. A comparative biocompatibility study of chondrocyte-derived ECM and silk fibroin scaffolds in vitro and in rat acute traumatic brain injury. Tissue Eng. Regen. Med. 6, 1420–1428.

Kim, M.S., Ahn, H.H., Cho, M.H., Shin, Y.N., Khang, G., Lee, H.B., 2007a. An in vivo study of the host tissue response to subcutaneous implantation of PLGA- and/or porcine small intestinal submucosa based scaffolds. Biomaterials 28, 5137–5143.

Kim, S.H., Choi, B.S., Ko, Y.K., Ha, H.J., Yoon, S.J., Rhee, J.M., Kim, M.S., Lee, H.B., Khang, G., 2007b. The characterization of PLGA/small intestinal submucosa composites as scaffolds for intervertebral disc. Key Eng. Mater. 342, 389–392.

Kim, M.S., Lee, S.J., Lee, H.B., Shin, H.W., Kim, S.H., Khang, G., 2006. Preparation and characterizations of porcine small intestinal submucosa sponge. Adv. Exp. Med. Biol. 585, 209–222.

Kranz, H., Ubrich, N., Maincent, P., Bodmeier, R., 2000. Physicomechanical properties of biodegradable poly(D, L-lactide) and poly(D, L-lactide-co-glycolide) films in the dry and wet states. J. Pharm. Sci. 89, 1558–1566.

Pollack, S.V., 1999. Some new injectable dermal filler materials: hylaform. Restylane, and artecoll. J. Cutan. Med. Surg. 3, S27–S35.

Ruozi, B., Parma, B., Croce, M.A., Tosi, G., Bondioli, L.V., Susannal, F.F., Vandelli, M.A., 2009. Collagen-based modified membranes for tissue engineering: Influence of type and molecular weight of GAGs on cell proliferation. Int. J. Pharm. 378, 108–115.

Shegokar, R., Müller, R.H., 2010. Nanocrystals: industrially feasible multifunctional formulation technology for poorly soluble actives. Int. J. Pharm. 399, 129–139.

Tiwari, A.K., Gajbhiye, V., Sharma, R., Jain, N.K., 2010. Carrier mediated protein and peptide stabilization. Drug Deliv. 17, 605–616.

Uebersax, L., Merkle, H.P., Meinel, L., 2009. Biopolymer-based growth factor delivery for tissue repair: from natural concepts to engineered systems. Tissue Eng. Part B Rev. 15, 263–289.

Wallace, D.G., Rosenblatt, J., 2003. Collagen gel systems for sustained delivery and tissue engineering. Adv. Drug. Deliv. Rev. 55, 1631–1649.

Yang, H.S., Seo, J.H., Kim, B.S., 2009. Serial propagation of cells on thermo-sensitive microcarrier. Tissue Eng. Regen. Med. 6, 1262–1267.

Ye, M., Kim, S., Park, K., 2010. Issues in long-term protein delivery using biodegradable microparticles. J. Contr. Rel. 146, 241–260.

Yu, L., Ding, J., 2008. Injectable hydrogels as unique biomedical materials. Chem. Soc. Rev. 37, 1473–1481.